PHYSICAL REVIEW B **84**, 161401(R) (2011)

Nanostructured graphene for energy harvesting

Miquel López-Suárez,[1] Riccardo Rurali,[2,*] Luca Gammaitoni,[3] and Gabriel Abadal[1]

[1]*Departament d'Enginyeria Electrònica, Universitat Autònoma de Barcelona, E-08193 Bellaterra, Barcelona, Spain*

[2]*Institut de Ciència de Materials de Barcelona (ICMAB–CSIC), Campus de Bellterra, E-08193 Bellaterra, Barcelona, Spain*

[3]*NiPS Laboratory, Dipartimento di Fisica, Universitá di Perugia, and Istituto Nazionale di Fisica Nucleare, Sezione di Perugia, I-06100 Perugia, Italy*

(Received 1 August 2011; revised manuscript received 12 September 2011; published 6 October 2011)

Engineered nonlinearities have been shown to play an important role in increasing the efficiency of energy harvesting devices. Macroscopic prototypes using this approach have been demonstrated recently [F. Cottone, H. Vocca, and L. Gammaitoni, Phys. Rev. Lett. **102**, 080601 (2009).] Here, in order to implement such a scheme at the nanoscale, we propose a simple device which is based on strained nanostructured graphene and discuss how it can respond to many energy sources that, although having a low intensity, are freely available, such as ambient vibrations or thermal noise. We discuss in some detail the case of thermal fluctuations harvesting in the steady-state nonequilibrium regime and of ambient vibrations.

DOI: 10.1103/PhysRevB.84.161401 PACS number(s): 61.48.Gh, 05.40.Ca, 05.10.Gg, 81.05.ue

An efficient power supply for increasingly small electronic devices is a challenging task that could prevent prototype nanocircuitry to move to mass production. On the other hand, as the size of devices shrinks, their power requirements also diminish.[1] Hence, energy sources that are freely available, such as ambient vibrations or thermal energy, become important and allow envisaging a batteryless world of self-powered devices.[2–5] For this reason, and to pursue clean energy sources compatible with a sustainable development, energy harvesting and energy conversion have become a very intense field of research.[6–9]

Linear mechanical resonators are the most common solution to convert vibrational into electrical energy[10,11] exploiting piezoelectric[7] or capacitive transduction.[12] Unfortunately, it is not always possible to tune their resonant frequency in the spectral region of ambient vibrations and, even when such tuning is possible, their efficiency rapidly decreases when moving away from the resonant frequency, which is an important limitation especially for broad spectral densities such as those of ambient vibrations. Cottone *et al.*[13] have demonstrated the role of engineered nonlinearity to improve significantly the efficiency of noise harvesting devices. Their macroscopic toy model consists of an inverted pendulum with a magnet attached to its tip. The approach of an external magnet is used to control the pendulum dynamics, pushing its tip away from its equilibrium position and making it oscillate around two unique and symmetric equilibrium positions. The magnetic repulsion can be tuned in a way that the pendulum operates as a bistable device, combining high-frequency oscillations around one of the two equilibrium positions—where it spends most of the time—with low-frequency, large excursions from one to the other.

In this Rapid Communication we show that a compressed graphene sheet can be used to implement such a bistable device to harvest thermal fluctuations and ambient vibrations at the nanoscale. The degree of compression ϵ is the only control parameter and allows switching among three possible regimes: (a) single-well potential ($\epsilon \sim 0$), (b) double-well potential with allowed swings from one minimum to the other (intermediate ϵ), i.e., the bistable device, and (c) double-well potential with no commutation between the two equilibrium positions (large ϵ). Yet, we show that graphene possesses an intrinsic nonlinearity[14] and can harvest thermal fluctuations and other kinds of nonequilibrium noise, outperforming any comparable linear oscillator, even when it is not compressed (see, for instance, Ref. 15 for general nonlinear potentials).

Thermal fluctuations are ubiquitously present in every dissipative system at a finite temperature. In principle, random fluctuations in equilibrium with their surroundings cannot be harvested without violating the second law of thermodynamics. However, it has been argued that equilibrium, a concept derived from macroscopic physics, is elusive when applied to the atomic scale and fluctuations become important.[16] Nevertheless, to avoid formal problems related to the definition of thermodynamical equilibrium of a nanoscale system, we restrict our discussion to the case of open systems in the steady-state nonequilibrium regime or systems under slowly varying local equilibrium conditions.

To calculate the deformation potential of graphene, we perform first-principles electronic structure calculations within density-functional theory (DFT). We use the SIESTA package,[17] norm-conserving pseudopotentials, and the generalized gradient approximation[18] to the exchange-correlation energy. Given the very large number of atoms necessary to describe the deformation that oscillating graphene undergoes, we use a minimal basis set, though for short graphene strips satisfactory convergence tests have been carried out against a more reliable single-ζ polarized basis. We obtain a Young's modulus of 0.85 TPa (assuming an effective thickness of the graphene sheet of 3.34 Å) and a Poisson ratio of 0.18. The structures were relaxed until all the forces were lower than 0.04 eV/Å, except for those atoms that need to be constrained to sample the transition states. To keep the computational load at a manageable level, rather than nanoribbons, we consider infinite graphene, which can be modeled by one single primitive cell along the y axis, the direction perpendicular to the deformation (see Fig. 1). The energy of a device with a given width W is obtained by rescaling the calculated energy by a factor W/w, w being the width of the primitive cell. It should be stressed that within this approximation, where a linear scaling of the

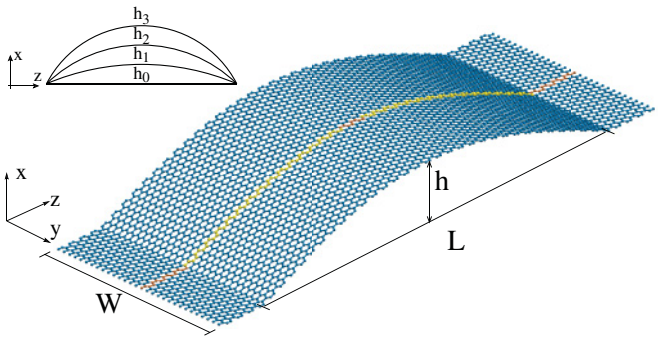

FIG. 1. (Color online) Buckled ground-state configuration of a graphene sheet under compressive strain. The atoms of the primitive cell explicitly introduced in the calculation within periodic boundary conditions are shown in light yellow (light gray). Atoms of the computational cell that need to be constrained to sample transition states (at the apex and at the clamped ends) are displayed with a darker color (gray). The potential profile is obtained by performing a series of calculations of sinusoidal deformations with increasing amplitudes h_i, as shown schematically in the inset.

energy with W is assumed, edge effects are neglected. Edges can generate stress fields, induce the formation of ripples and, in general, will affect the overall dynamic behavior of the system. These effects are not accounted for in our model. However, for the width of ribbons to be used in realistic devices the energetics and the dynamic response of the system is not expected to qualitatively change.

We start from a flat graphene sheet with a compressive strain ϵ [defined as $(L_0 - L)/L_0$, where L is the length of the graphene sheet and L_0 its equilibrium value in absence of compression; see also Fig. 1] ranging from 0% to 0.1%. For each value of ϵ we generate several sinusoidal deformations with an increasing amplitude h_i (see the inset of Fig. 1). Previous tests indicated that sinuslike profiles are close to the minimum energy configurations, and thus are good initial guesses. Next, we carry out a geometric optimization of each structure. Small regions at the beginning and at the end of the strip are kept flat to mimic typical nanoindentation experiments. As our purpose is mapping the potential landscape, the apex of each of the deformed strip is kept fixed to prevent all the structures from relaxing to their atomic ground state.

As illustrated in Fig. 2, the potential has a minimum at $h = 0$ in the case of uncompressed graphene, while for $\epsilon > 0$ two symmetric minima appear, indicating that graphene favors a buckled configuration such as the one sketched in Fig. 1. As ϵ increases, the minima move apart and the transition barrier grows, making the commutation between wells less likely.

The dynamics of the system is described by the equation of motion

$$m\ddot{x} = -\frac{\partial E_p}{\partial x} - b\dot{x} + F_0\xi(T), \tag{1}$$

where E_p is the elastic (potential) energy as obtained by the electronic structure calculations and reported in Fig. 2. As customary in the study of beam deflection or cantilever vibrations, we reduce the dynamics of the clamped graphene sheet of total mass M to the equivalent dynamics of a free pointlike mass $m = 0.4M$.[19] Here we assume a simple phenomenological viscous damping term[20] with a damping coefficient that in the harmonic potential case can be expressed as $b = m\omega_0/Q$, taking $Q = 100$ for the quality factor of a graphene sheet in air. In general the mechanical dissipation in the graphene dynamics is due to a number of different phenomena[21,22] and can be more properly expressed in terms of a dissipation function that takes into account generalized memory effects as in the expression $\int_{-\infty}^{t} b(t-\tau)\dot{x}(\tau)d\tau$.

$F_0\xi(T)$ represents the random force [$\xi(T)$ is a flat spectrum stochastic process, Gaussian distributed, with zero mean and unitary standard deviation] accounting for the thermal noise-induced stochastic dynamics of the graphene sheet. When the potential is harmonic ($E_p = 1/2kx^2$) and the system is at thermal equilibrium, the fluctuation-dissipation theorem links the magnitude of the thermal fluctuation to the damping coefficient via $\hat{F}_0^2 = 4k_BTb$, where k_B is the Boltzmann

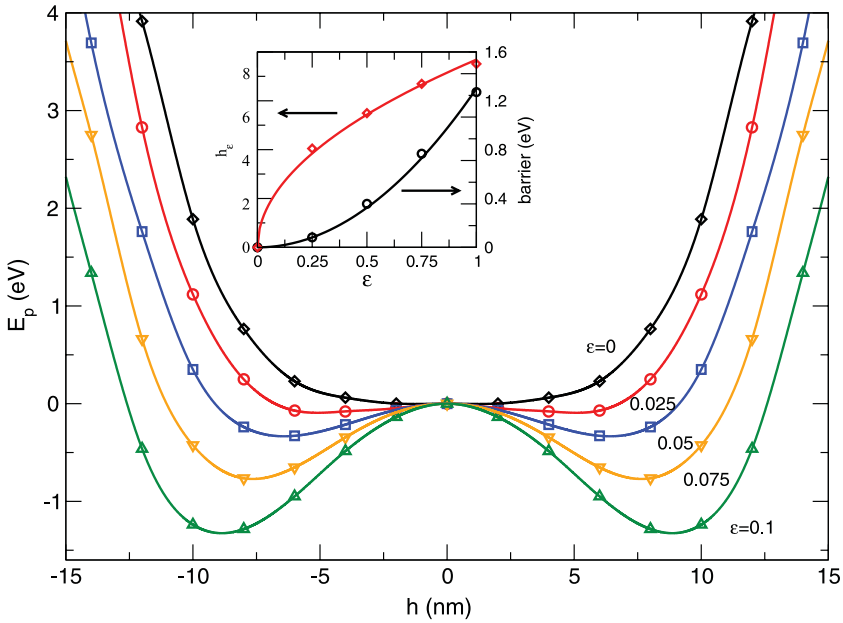

FIG. 2. (Color online) Potential as a function of the out-of-plane coordinate h for compressions ϵ ranging from 0% to 0.1%. Finite values of ϵ favor buckling of the graphene sheet, with two symmetric minima at $h \neq 0$. The inset displays the separation between the minima and the transition barrier as a function of ϵ, together with fits to ϵ^2 and $\sqrt{\epsilon}$, respectively.

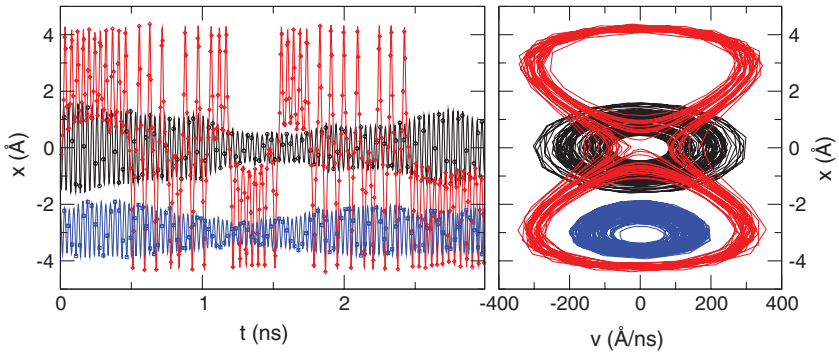

FIG. 3. (Color online) Evolution of the position x in the three possible regimes: (i) At low applied compressions the system oscillates in a single-well potential at approximately $x = 0$ (black circles); (ii) at the optimal compression a bistable behavior is clearly observed, with long swings from one well to the other (red diamonds); (iii) at large compressions the buckled graphene gets trapped in one of the minima (blue squares). The left-hand panel shows the time evolution $x = x(t)$; the right-hand panel is the attractor diagram $x = x(v)$.

constant and T is the temperature. In this case the root mean square (rms) of the displacement amounts to $x_{\rm rms} = \sqrt{k_B T/k}$.

The potential that we obtained from the DFT calculations, however, is strongly nonharmonic, even in the simple case of uncompressed graphene, where a satisfactory fit is achieved only with the order-4 polynomial $c_4x^4 + c_2x^2$ (we obtain $c_4 = 0.12$ meV Å^{-4} and $c_2 = 6.59$ meV Å^{-2} for the nanoribbon of Fig. 2). Hence a useful prediction from the stochastic differential equation (1) can only be obtained numerically. Here we used the well-known Euler-Maruyama method, where the stochastic force intensity is set arbitrarily at $\hat{F}_0^2 = 4k_BTb$ with a flat spectral distribution (white noise approximation) and $T = 300$ K, to mimic a nonequilibrium thermal noise acting on the graphene sheet.

Solutions of Eq. (1) for a graphene nanoribbon of 1×17 nm are shown in Fig. 3 for the different working regimes. This graph illustrates how the dynamics of the system can be controlled by tuning the level of compression. At high values of ϵ the trajectory is confined around one of the two attractors, in a buckled configuration, whereas for low ϵ the barrier is not effective and the system is swinging in a perturbed, single-well potential around zero. It is at intermediate compressions that the system can jump from one well to the other, increasing the rms of the position vector. This optimal compression range

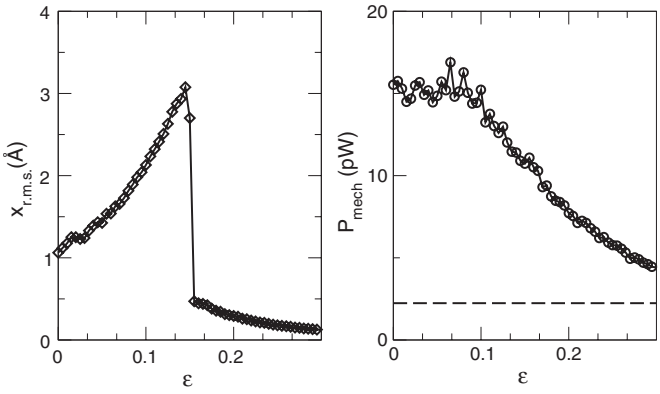

FIG. 4. Root mean square (rms) of the position vector x (left-hand side) and mechanical power (right-hand side) as a function of the compressive strain ϵ. The optimal compression that maximizes $x_{\rm rms}$ is $\epsilon \sim 0.17$. This value of ϵ also maximizes the piezoelectrically generated voltage in the transduction circuit described in the text. The dashed line in the right-hand panel gives an estimation of the mechanical power accumulated by a linear oscillator of comparable size to the one discussed.

depends on the geometrical parameters of the graphene device and the temperature of the noise that has to be harvested.[13]

The dependence of $x_{\rm rms}$ on the compression level is shown in Fig. 4(a). Here the $x(t)$ time series has been averaged to zero before computing the $x_{\rm rms}$ in order to filter out any dc component that cannot be considered interesting for energy harvesting purposes as in Ref. 13. Increasing ϵ leads to an increase of the rms of the position: The two attractors of the dynamics have appeared, but the barrier still allows low-frequency swings from one well to the other. At approximately $\bar{\epsilon} = 0.17$, $x_{\rm rms}$ gets to a maximum and then drops dramatically, indicating that the barrier has reached a critical value and the dynamics is trapped in one of the two attractors.

The mechanical power, defined as $P_{\rm mech} = \langle F_0\xi(T)\dot{x}\rangle$, on the other hand, is slowly decaying and does not present a maximum at $\bar{\epsilon}$ [see Fig. 4(b)]. This happens because, although the graphene sheet on average moves *more*, as shown in Fig. 4(a), it also moves *slower*, yielding a decrease in the mechanical power.[23]

Figure 4(b) seems to suggest that it is pointless to pursue the double-well potential of the buckled graphene, because the maximum mechanical power is accumulated by flat graphene. However, as it will be clear in the following, in order to harvest electrical energy we need a conversion mechanism that is capable of transforming the available mechanical energy into this final form of energy. Before dealing with the conversion mechanism, we further note that another energy source that could be scavenged is represented by ambient vibrations, such as mechanical vibrations and acoustic energy,[3,4,24] that are not intrinsic to the system as is the thermal noise considered so far. The main limitation of conventional linear nano-oscillators with respect to these kinds of environmental vibrations is the poor flexibility of their frequency sensitivity: Not only is the spectral response usually very narrow, but it is also difficult to shift it toward the low-frequency domain, which is where most of the ambient vibration energy is located.

The spectral response of the proposed graphene device, expressed by the vector $X(\omega) = \mathcal{F}\{x(t)\}$, is shown in Fig. 5. The output spectrum shown represents the amplitude of movement in response to each frequency component of the incident noise. Indeed, the larger average mechanical power is harvested by the flat graphene [Fig. 4(b)], but responds only to frequencies close to a resonance frequency of ~30 GHz, with an approximate bandwidth of 10 GHz. On the other hand, close to the optimal compression, when the system is allowed to swing from one well to the other, a very broad range of

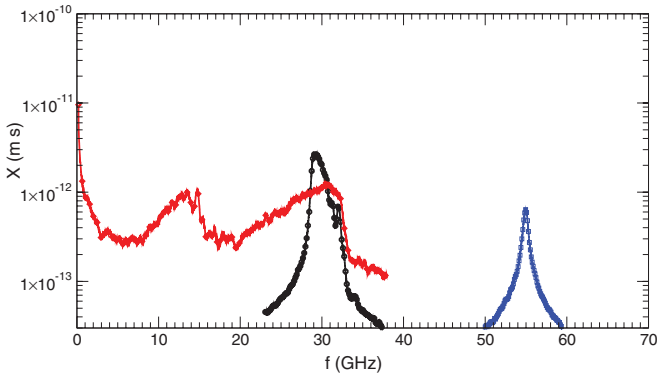

FIG. 5. (Color online) Spectral response in the three operating regimes. Zero or too large compressive strains yields rather selective frequency responses (black circles and blue squares, respectively). Around the optimal compression, on the other hand, the spectral response is much broader and extends significantly to the low-frequency domain (red diamonds). The spectral response is defined as the Fourier transform of the position vector as follows: $X(\omega) = \mathcal{F}\{x(t)\} = \frac{1}{\sqrt{2\pi}} \int_{-\infty}^{+\infty} x(t) e^{-i\omega t}\, dt$.

frequencies can be harvested, with a noticeable extension to low frequencies. This means that even if the maximum power is higher in the uncompressed case [$P(\bar{\epsilon})$ is 2/3 of the maximum power $P(0)$], the device becomes sensitive to a much broader frequency spectrum, with an integrated power that exceeds significantly the linear case, especially in the case of harvesting ambient vibrations. It should be noticed that when the optimal compression is exceeded and the system gets stuck in one of the two wells, the spectral response gets significantly worse, resulting in a narrower and higher-frequency distribution, even with respect to the case of flat graphene. This fact suggests that certain caution should be paid when choosing the value of ϵ, especially in view of the experimental difficulties to control it with accuracy.

The energy harvested by the vibrating graphene device, however, cannot be stored in a simple way, as mechanical energy storing is an elusive task and a very intense research field. Yet, the harvested thermomechanical energy needs to be converted to electrical energy and used immediately or stored with known storing procedures, namely, through electrical capacitors. As we discuss below, such a conversion provides an argument in favor of the buckled configuration.

Devising and engineering an efficient transduction scheme is subjected to the optimization of many parameters. Here we assume a simplified piezoelectric conversion model consisting of two ZnO transducers placed at the clamped ends of the suspended sheet. The behavior of the piezoelectric material is modeled as a capacitance with a deformation-dependent charge density $d_{31} = -5.1 \times 10^{-12}$ m/V,[25,26] coupled to a load resistance. Following Roundy and Wright,[11] the whole dynamics of the graphene harvester can be described by

$$m\ddot{x} = -\frac{\partial E_p}{\partial x} - b\dot{x} - \Gamma_1 V + F_0 \xi(T), \tag{2}$$

$$\dot{V} = \Gamma_2 \dot{x} - \frac{V}{RC}, \tag{3}$$

where the motion equation is modified by the inclusion of a piezoelectric term [Eq. (3)], which accounts for the forces associated with the transduction mechanism and which couples motion and the transduction equations [Eq. (3)]. Taking a large enough value of the time constant RC of the transducing circuit (low cut-on frequency $\omega_{hp} = 1/RC$), the second equation provides $V = \Gamma_2 x$, where V is the generated voltage and Γ_2 is the electromechanical coupling coefficient as defined in Ref. 11. Therefore, the piezoelectric rms voltage V is simply the rms of the position vector rescaled by a factor Γ_2—taken to be 5.8 V/m from Ref. 11. Now the maximum harvested electrical power $P_{\rm el} = V^2/R$ no longer corresponds to the unstrained graphene sheet and the optimal compression is $\bar{\epsilon}$, the one that gives the larger $x_{\rm rms}$ (see Fig. 4), as previously observed in Ref. 13. This piezoelectric model is admittedly a simple one, and it should be taken into account that the specific transduction scheme implemented will also affect the overall dynamics of the system.

In conclusion, we have shown that a nanostructured graphene device can harvest ambient noise thanks to its intrinsically anharmonic deformation potential, outperforming conventional linear oscillators. A linear oscillator of a size comparable to our device is estimated to harvest 2.2 pW of mechanical power, almost one order of magnitude less than flat graphene. Under an appropriate compressive strain the graphene sheet assumes a buckled configuration and behave as a bistable device. Such an engineered nonlinearity is shown to broaden the spectral response, extending it toward the low-frequency domain, where most of the ambient energy source is typically available. Mechanical-to-electrical energy conversion through a model piezoelectric transduction scheme is briefly discussed.

L.G. acknowledges financial support of the Future and Emerging Technologies (FET) programme of the European Commission (FPVII, Grant Agreement No. 256959, NANOPOWER and Grant Agreement No. 270005, ZEROPOWER). Funding under Contract Nos. TEC2009-06986, FIS2009-12721-C04-03, CSD2007-00041, and ENE2009-14340-C02-02 are greatly acknowledged.

*rrurali@icmab.es

[1] E. Pop, Nano Rese. **3**, 147 (2010).
[2] J. Song, J. Zhou, and Z. L. Wang, Nano Lett. **6**, 1656 (2006).
[3] X. Wang, J. Song, J. Liu, and Z. L. Wang, Science **316**, 102 (2007).
[4] S. P. Beeby, M. J. Tudor, and N. M. White, Meas. Sci. Technol. **17**, R175 (2006).
[5] S. Roundy, J. Intell. Mater. Syst. Struct. **16**, 809 (2005).
[6] J. Paradiso and T. Starner, IEEE Pervasive Comput. **4**, 18 (2005).
[7] Z. L. Wang and J. Song, Science **312**, 242 (2006).
[8] K. A. Cook-Chennault, N. Thambi, M. A. Bitetto, and E. Hameyie, Bull. Sci. Technol. Soc. **28**, 496 (2008).

[9]V. Balzani, A. Credi, and M. Venturi, Chem. Soc. Rev. **38**, 1542 (2009).

[10]S. Meninger, J. Mur-Miranda, R. Amirtharajah, A. Chandrakasan, and J. Lang, IEEE Trans. Very Large Scale Integration (VLSI) Syst. **9**, 64 (2001).

[11]S. Roundy and P. K. Wright, Smart Mater. Struct. **13**, 1131 (2004).

[12]P. A. Truitt, J. B. Hertzberg, C. C. Huang, K. L. Ekinci, and K. C. Schwab, Nano Lett. **7**, 120 (2007).

[13]F. Cottone, H. Vocca, and L. Gammaitoni, Phys. Rev. Lett. **102**, 080601 (2009).

[14]E. Cadelano, P. L. Palla, S. Giordano, and L. Colombo, Phys. Rev. Lett. **102**, 235502 (2009).

[15]L. Gammaitoni, I. Neri, and H. Vocca, Appl. Phys. Lett. **94**, 164102 (2009).

[16]C. Jarzynski, Séminaire Poincaré XV Le Temps, p. 77 (2010).

[17]J. M. Soler, E. Artacho, J. D. Gale, A. García, J. Junquera, P. Ordejón, and D. Sánchez-Portal, J. Phys. Condens. Matter **14**, 2745 (2002).

[18]J. P. Perdew, K. Burke, and M. Ernzerhof, Phys. Rev. Lett. **77**, 3865 (1996).

[19]V. Kaajakari, *Practical MEMS* (Small Grid Publishing, Las Vegas, NV, 2009).

[20]J. Atalaya, A. Isacsson, and J. M. Kinaret, Nano Lett. **8**, 4196 (2008).

[21]J. S. Bunch, A. M. van der Zande, S. S. Verbridge, I. W. Frank, D. M. Tanenbaum, J. M. Parpia, H. G. Craighead, and P. L. McEuen, Science **315**, 490 (2007).

[22]C. Seoánez, F. Guinea, and A. H. Castro Neto, Phys. Rev. B **76**, 125427 (2007).

[23]Upon compression the potential energy of the graphene sheet grows, thus its kinetic energy has to decrease.

[24]T. Galchev, H. Kim, and K. Najafi, Procedia Chem. **1**, 1439 (2009).

[25]F. Bernardini, V. Fiorentini, and D. Vanderbilt, Phys. Rev. B **56**, R10024 (1997).

[26]M.-H. Zhao, Z.-L. Wang, and S. X. Mao, Nano Lett. **4**, 587 (2004).